Electronic Supplementary Material (ESI) for Soft Matter

Supplementary Information

Conformational Analysis of Single Polymer Chains in Three Dimensions by Super-resolution Fluorescence Microscopy

Hiroyuki Aoki,[1,2,*] Kazuki Mori,[2] Shinzaburo Ito[1,2]

Advanced Biomedical Engineering Research Unit[1] and Department of Polymer Chemistry[2], Kyoto University, Nishikyo, Kyoto 610-8510, Japan

Synthesis of rhodamine spiroamide derivative

3',6'-bis(diethylamino)-2-(2-hydroxyethyl)-2,3-dihydrospiro[isoindole-1,9'-xanthene]-3-one (RSA-OH). Rhodamine B hydrochloride (3.9 g, 8.1 mmol, Wako Pure Chemical Industries, Osaka, Japan) and 2-aminoethanol (6.0 mL, 100 mmol, Nacalai Tesque, Kyoto, Japan) was dissolved in 35 mL of distilled dimethylformamide (DMF, Wako Pure Chemical Industries) in a three-necked round bottom flask under a nitrogen atmosphere, then 5.0 mL (36 mmol) of triethylamine (Wako Pure Chemical Industries) and 5.0 g (13 mmol) of *o*-(7-azabenzotriazol-1-yl)-*N*,*N*,*N*',*N*'-tetramethluronium (HATU) (Tokyo Chemical Industry, Tokyo, Japan) were added. The reaction mixture was stirred for 40 h at 40 °C. The product was purified by a silica gel chromatography with an eluent

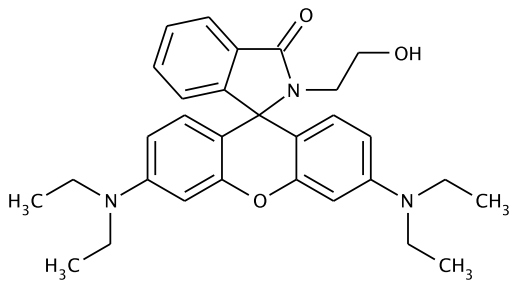

of dichloromethane/methanol (10/1, v/v), affording 3.0 mg of a pale pink product (yield: 75 %). The product was soluble to methanol, ethanol, acetone, toluene, chloroform, dichloromethane, dichloroethane, and DMF. Elemental analysis: C 74.1, H 7.26, O 9.89, N 8.64 (found); C 74.2, H 7.26, O 9.89, N 8.65 (calcd). ^{1}H NMR (400 MHz, $CDCl_3$): δ = 1.17 (t, J = 6.9 Hz, 12H), 3.27-3.36 (m, 10H), 3.47 (dd, J = 9.6, 5.0 Hz, 2H), 4.17 (s, 1H), 6.29 (dd, J = 8.8, 2.2 Hz, 2H), 6.38 (d, J = 2.2 Hz, 2H), 6.49 (d, J = 8.8 Hz, 2H), 7.07 (t, J = 4.1 Hz, 1H), 7.43–7.46 (m, 2H), 7.90 (t, J = 4.1 Hz, 1H). Melting point: 215°C.

2-[3',6'-bis(diethylamino)-3-oxo-2,3-dihydrospiro[isoindole-1,9'-xanthene]-2-yl]ethyl 2-methylprop-2-enoate (RSA-MA). Methacryloyl chloride (0.60 mL, 6.2 mmol, Tokyo Chemical Industry) was dissolved in 2.0 mL of 1,2-dichloroethane (DCE, Wako Pure Chemical Industries), and it was added dropwise to a DCE solution (8.0 mL) of RSA-OH (1.0 mg, 2.1 mmol) and pyridine (0.5 mL, 6.2 mmol, Wako Pure Chemical Industries) at 0°C. After 60 min of stirring, the temperature was gradually raised to 20°C, and then the reaction was kept for 24 h at a room temperature. After the reaction mixture was washed with water, the solvent was evaporated. After the silica gel chromatography with an eluent of dichloromethane/methanol (40/1, v/v), 440 mg of the final product RSA-MA was obtained as a pale pink powder (Yield: 38 %). The solubility of the obtained RSA-MA was similar to that of RSA-OH. Elemental analysis: C 73.5, H 7.10, O 11.8, N 7.60 (found); C 73.8, H 7.08, O 11.5, N 7.59 (calcd). ^{1}H NMR (400 MHz, $CDCl_3$): δ = 1.16 (t, J = 7.0 Hz, 12H), 1.84 (s, 3H), 3.33 (q, J = 7.1 Hz, 8H), 3.49 (t, J = 6.6 Hz, 2H), 3.80 (t, J = 6.5 Hz, 2H), 5.47 (s, 1H), 5.99 (s, 1H), 6.25 (dd, J = 8.9, 2.6 Hz, 2H), 6.37 (d, J = 2.4 Hz, 2H), 6.44 (d, J = 9.0 Hz, 2H), 7.06 (t, J = 4.3 Hz, 1H), 7.41–7.44 (m, 2H), 7.91 (t, J = 4.3 Hz, 1H). Melting point: 83°C.

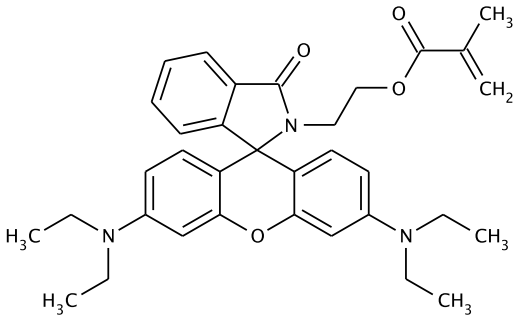

Polymerization. Poly(alkyl methacrylate)s labeled with the photochromic rhodamine spiroamide were synthesized by the atom transfer radical copolymerization of RSA-MA and alkyl methacrylate monomers: methyl methacrylate, butyl methacrylate, and hexyl methacrylate (Wako Pure Chemical Industries). The monomers were washed with an aqueous solution of NaOH to remove the polymerization inhibitor and distilled under reduced pressure before use. The mixture of a methacrylate monomer, RSA-MA, and *p*-toluenesulfonyl chloride (Tokyo Chemical Industry) was degassed by three freeze-pump-thaw cycles in a glass tube. A degassed anisole solution of CuCl(I) and 4,4'-dinonyl-2,2'-dipyridyl (Sigma-Aldrich, St. Louis, MO, USA) was added to the monomer mixture under vacuum. The polymerization was carried out at 70°C and quenched by cooling at 0°C. After the polymerization, the high molecular weight component was separated by the fractional reprecipitation with toluene and methanol. The weight- and number-average molecular weights (M_w and M_n, respectively) were evaluated by size exclusion chromatography (KF-806L, Shodex, Tokyo, Japan) calibrated with poly(methyl methacrylate) and poly(butyl methacrylate) standards (Polymer Standards Service, Mainz, Germany). The RSA fraction of the labeled polymer was evaluated to be 0.78% from the ratio of the peak areas attributed to the protons of the RSA moiety and the alkyl group in ^{1}H NMR spectra (JNM-EX400, JEOL, Tokyo, Japan). The labeled PBMA showed the same thermal and mechanical properties as the unlabeled polymer, and the phase separation was not observed for the blends of the labeled and unlabeled PBMA. This indicates that the properties of PBMA was not influenced by the introduction of the dye moiety at the fraction of 0.78%.

Apparatus

The PALM set-up consisted of an inverted microscope (TE-2000, Nikon, Tokyo, Japan), an electron-multiplying charge-coupled device (EMCCD) camera (iXon+ DU-897, Andor Technology, Belfast, Ireland), and laser light sources. In order to trigger the isomerization reaction of RSA, a 378-nm laser was employed (LDM-375, Oxxius, Lannion, France).

The fluorescence image of the open-form isomer was excited at a wavelength of 532 nm (MGL-III-532, CNI, Changchun, China). The 378- and 532-nm beams were colinearly overlapped by a dichroic mirror (LM01-503-25, Semrock, Rochester, NY, USA) and focused on a back focal plane of a 100× microscope objective (UPLSAPO 100XO, Olympus, Tokyo, Japan). The fluorescence signal from the dye molecule in the open-form isomer was imaged on the EMCCD camera with the pixel binning of 2 × 2 through a dichroic mirror (LPD01-532RS-25x36x1.1, Semrock), a long-pass filter (BLP01-532R-25, Semrock), and a 2.5× magnifier lens. The image acquisition was carried out at a camera exposure time of 10 ms and a frame interval time of 30 Sms. The UV beam for the activation was in pulsed operation synchronized with the interval of the exposure time for each frame to avoid the autofluorescence from the sample and the optical system. The illumination dose of the activation laser during the camera exposure was controlled by the length of the UV pulse in the range of 0.02 – 8 ms at a power density of 0.8 kW/cm^2. The excitation illumination at 532 nm was also synchronized with the camera exposure time. The synchronization was performed by TTL signals from the EMCCD camera through a pulse generator (9614+, Quantum Composers, Bozeman, MT, USA). In the three-dimensional astigmatic imaging, a cylindrical lens with a focal length of 10 m (CVI Melles Griot, Albuquerque, NM, USA) was inserted before the tube lens in the microscope.

PALM analysis

Each fluorescence spot for a dye molecule was fitted to a two-dimensional Gaussian function to determine the xy coordinate (x_0, y_0):

$$I(x,y) = I_0 \exp\left(-\frac{(x-x_0)^2}{w_x^2} - \frac{(y-y_0)^2}{w_y^2}\right), \tag{S1}$$

where $I(x,y)$ is the intensity at the position (x,y) in the fluorescence image, and w_x and w_y are the width of the fluorescence spot in the x- and y-directions. The fitting was conducted for the fluorescence spot with the photon number of more than 2000. The localization accuracy was examined by the standard deviation of the fitting results for 300 independent images for a single dye molecule. In the three-dimensional observation, a dye molecule

was observed in an ellipsoidal shape due to the astigmatism due to the cylindrical lens put in front of the tube lens of the microscope. The ellipticity and the direction of the observed elliptical spot are dependent on the z-coordinate of the molecule, z. Now we define a shape parameter, E, as a function of z.

$$E = \frac{w_x - w_y}{w_x + w_y} \tag{S2}$$

The relationship between the z-coordinate and the shape parameter was calibrated by the observation of a single rhodamine B molecule at different height positions. The fluorescence images of the molecule were acquired with moving the sample in the z-direction from –500 to 500 nm with a step distance of 10 nm (the origin was defined as the point where a molecule was observed spherically) by a piezo-driven three-dimensional translation stage (P-733.3DD, Physik Instrumente, Karlsruhe, Germany).

The localization accuracy of a single molecule was 15 nm in the two-dimensional PALM measurement. The super-resolution image was reconstructed by plotting two-dimensional Gaussian functions at the obtained molecule positions, the standard deviation of which were 15 nm. The pixel size of the reconstruction image was 5×5 nm^2. In the three-dimensional imaging with the cylindrical lens, the localization accuracy in the lateral dimensions was asymmetric because of the different width in the x- and y-directions of a single molecule observed in an ellipsoidal shape. Therefore, the width of the plotted spot was set to 20 nm, which was the greater value of the localization accuracy. In the localization accuracy in the z-direction was 40 nm. The super-resolution image was generated by putting the following Gaussian intensity distributions in a three-dimensional reconstruction space with a voxel size of $5 \times 5 \times 5$ nm^3.

$$I_i(x, y, z) = \exp\left(-\frac{(x - x_i)^2}{\sigma_x^2} - \frac{(y - y_i)^2}{\sigma_y^2} - \frac{(z - z_i)^2}{\sigma_z^2}\right), \tag{S3}$$

where $\sigma_x = \sigma_y = 20$ nm, $\sigma_z = 40$ nm, and (x_i, y_i, z_i) is the coordinate of the i-th molecule.

Translational diffusion of single PBMA chain

The fluorescence-labeled PBMA was prepared by the atom transfer radical polymerization of butyl methacrylate initiated from a mono-functional initiator having a perylene diimide (PDI) moiety. [1] Each chain was labeled by a single PDI molecule at a chain end. The weight-average molecular weight was 1.1×10^5 with the polydispersity index of 1.25. The labeled polymer was dispersed in a 200-nm-thick film of the unlabeled PBMA at a concentration of 10^{-6}. In the fluorescence imaging, the labeled chain was observed at an area density of about 0.1 chains μm^{-2}. The consecutive images were acquired for 60 min at 25°C with the camera exposure time of 100 ms with an interval time of 20 s. In this condition, the localization accuracy of a single PDI molecule was 8.5 nm.

Figure S1a shows a typical time trajectory of the x-coordinate of a single PBMA chain, indicating the fluctuation of the observed coordinate with the standard deviation of 8.8 nm. Figure S1b shows the relationship between the mean squared displacement (MSD) and time. This indicates that the MSD showed a constant value of about 160 nm^2 and it was not dependent on time. The finite value of MSD is due to the localization uncertainty of the single molecule observation. Thus, the translational diffusion of a chain segment of PBMA was negligible. It should be noted that the negligible diffusion was observed for

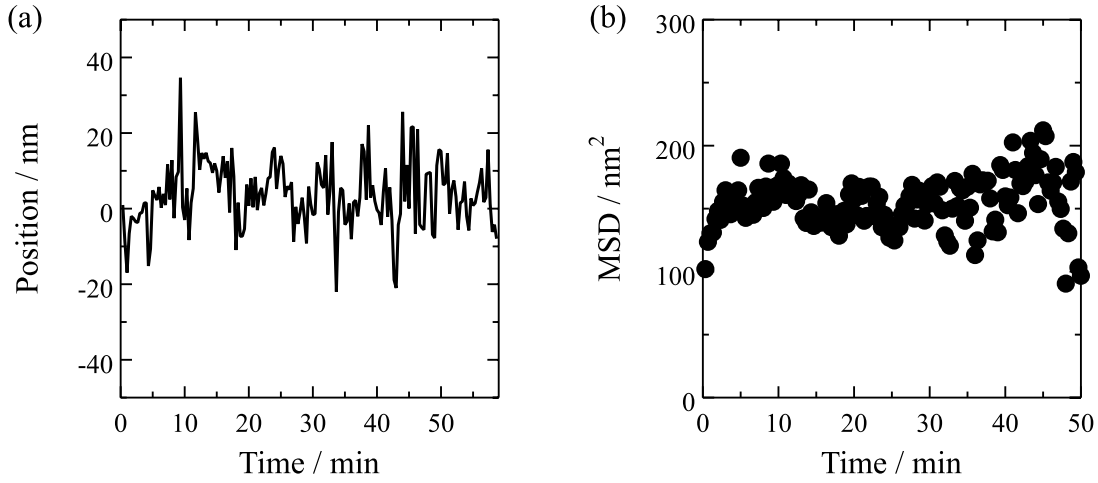

Figure S1. Time trajectory of the x-coordinate (a) and the mean squared displacement (b) for an end-labeled PBMA chain.

the molecular weight of 10^5, which is 20 times smaller than the sample polymer for the PALM imaging. The larger the molecular weight is, the slower the molecular motion is. Therefore, this result indicates that the labeled PBMA chain with the molecular weight of 2×10^6 showed negligible diffusion in the measurement time and that the observed PALM image was not blurred by the molecular motion.

Random-walk simulation

Random-walk chains with the unit length of L were generated in three dimensions. It should be noted that the second moment tensor $\mathbf{S}$ of Eq. 2 in the text is defined for the two-dimensional projection of each chain. Therefore, the simulated $\mathbf{S}$ was obtained using the x and y coordinates of the random-walk chain.

At first, we discuss the effect of the resolution on the observed chain dimension. As mentioned in the text, the coordinate of the labeled segments on the polymer chain was evaluated with a localization uncertainty of 15 nm. The error in the measurement of the coordinate of each segment may affect the evaluated value of R_g. In order to discuss this point, we performed the simulation considering the localization uncertainty as follows. A single random-walk chain with a step number of 5000 was generated, and 40 segments were randomly picked up, which corresponds to the labeled moieties along the chain. The tensor $\mathbf{S}$ was calculated by the coordinates of the 40 labeled segments. In order to introduce the localization uncertainty, the coordinate of each segment was altered by adding a random number having a normal distribution with a standard deviation of σ_{loc}. The apparent radius of gyration considering the localization uncertainty, R_σ, was evaluated by Eq. 2 in the text for the 10^5 alterations for the same chain conformation.

Figure S2a shows the histogram of R_σ for the random-walk chain with different σ_{loc} (the values of R_σ and σ_{loc} are normalized by the radius gyration without the uncertainty, R_0). For a given conformation, the localization uncertainty results in the dispersion of R_σ. This result also indicates that the average of R_σ is larger than R_0. Figure S2b shows the uncertainty effect on R_σ and the standard deviation of apparent radius of gyration, σ_R,

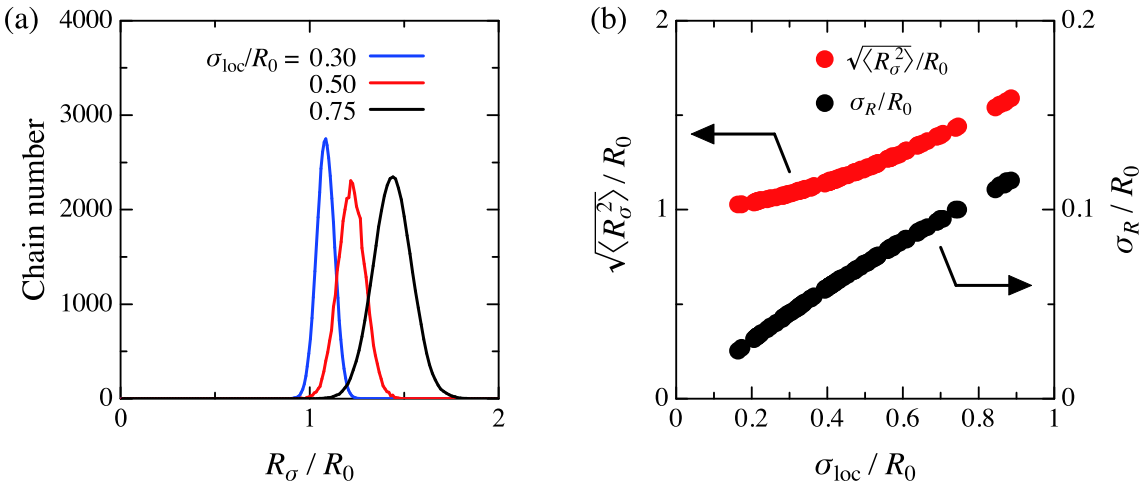

Figure S2. Relationship between the apparent chain dimension and the localization accuracy. (a) Histogram of R_σ for a given chain conformation. (b) Effect of localization uncertainty on R_σ and σ_R.

which is the result of the calculation for different 100 chain conformations. This indicates that the increase of the localization uncertainty results in the error in the evaluation of the chain dimension and the overestimation of $\sqrt{\langle R_\sigma^2 \rangle}$. However, the deviation was not large compared to R_0. For example, when the localization uncertainty is the half of the chain dimension ($\sigma_{loc} = R_0/2$), the error of the radius of gyration of a single chain, σ_R, is less than 7% and the overestimation of the average chain dimension is less than 20%. Now we consider the effect of the localization uncertainty in the actual length scale. In the experiment, the average chain dimension was 38 nm and the localization uncertainty was 15 nm. Considering the effect of the overestimation of the evaluated chain dimension from R_0, this corresponds to $\sigma_{loc}/R_0 = 0.47$. From Figure S2b, the standard deviation of the chain dimension for a single chain σ_R/R_0 is 0.068. Therefore, the accuracy of the evaluated chain dimension of a labeled PBMA chain can be estimated to be 2.5 nm.

In order to compare the simulation and the experiment, the effect of the molecular weight distribution should be considered. The labeled PBMA used as the sample showed the molecular weight distribution of 1.25 as shown in Figure S3 (the solid curve); therefore, the random-walk chains with different step numbers were generated. The step number distribution of the random-walk chain was the same as the molecular weight distribution

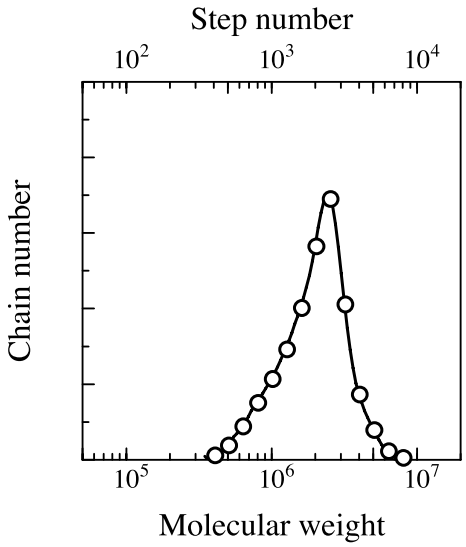

Figure S3. Size exclusion chromatogram of the labeled PBMA (solid curve) and the step number distribution of the simulated random-walk chain (open circles).

of the labeled PBMA as shown in Figure S3 (open circles). The total number of the generated chains was 10^6, and the radius of gyration and the asphericity were evaluated for each chain considering the localization uncertainty. For the comparison with the experimentally obtained R_g, the step length L of the random walk chain was scaled to give the same value of the root of the mean square radius of gyration as the experimental value of 38 nm.

References

[1] Aoki, H.; Takahashi, T.; Tamai, Y.; Sekine, R.; Aoki, S.; Tani, K.; Ito, S. *Polym. J.* **2009**, *41*, 778–783.